

## Comparison of Targeting Accuracy for Treatment Localization with Different CT Images of Moving Target in Thorax Region

Rattanaporn Sirichai BSc<sup>1</sup>, Benjamas Ngamching BSc<sup>1</sup>, Chirasak Khamfongkhrua MSc<sup>1</sup>,  
Sunanta Rojwatkarnjana MD<sup>1</sup>, Danupon Nantajit PhD<sup>2</sup>, Chirapha Tannanonta MSc<sup>1</sup>

<sup>1</sup> Department of Radiation Oncology, Chulabhorn Hospital, HRH Princess Chulabhorn College of Medical Science,  
Chulabhorn Royal Academy, Bangkok, Thailand

<sup>2</sup> Faculty of Medicine and Public Health, HRH Princess Chulabhorn College of Medical Science,  
Chulabhorn Royal Academy, Bangkok, Thailand

**Objective:** To compare the accuracy of four different reconstruction techniques of Computed Tomography [CT] images for localization of moving targets.

**Materials and Methods:** A respiratory motion phantom was simulated for tumor motion with the respiratory rate of 15 breaths per minute, breathing amplitude 1.0 cm in craniocaudal [CC] direction. In treatment room, the four different reconstruction of CT image: free breath [FB], maximum intensity projection [MIP], mid-position [MidP] and average intensity projection [AIP], were compared with the FB kV-Cone-Beam CT obtained from the on-board imaging system of TrueBeam linear accelerator. The accuracy of target localization was calculated in terms of mean deviation and matching index [MI]. Additionally, image quality and tumor shape were evaluated using visual grading analysis of 10 observers.

**Results:** The mean deviation of target position was significant in CC direction with the maximum value of  $3.11 \pm 0.65$  mm in the MidP images. The high MI values were 0.86 and 0.87 in AIP and FB images, respectively. Moreover, AIP and FB had high grading scores for both image quality and tumor shape.

**Conclusion:** Both FB and AIP image datasets can be used as the reference image for localizing the lung tumor with less than 2 cm movement in CC direction.

**Keywords:** 4DCT image acquisition, kV-CBCT, Moving target, Target localization

**J Med Assoc Thai 2018; 101 [Suppl. 6]: S119-S124**

**Website:** <http://www.jmatonline.com>

Respiration-induced tumor motion is a major obstacle for achieving high-precision radiotherapy of cancers in the thorax region because respiratory motion can generate artifacts for all imaging modalities leading to difficulties in clearly delineating boundaries<sup>(1)</sup>. One of the major challenges is tumor motion during treatment delivery that needs to be accounted for, so that large and focused radiation doses can be given. In

general, tumor motion is evaluated with combined information from fluoroscopic imaging<sup>(1-3)</sup>, slow computed tomography [CT] scans<sup>(1,4,5)</sup> and especially, four-dimensional CT scans [4DCT]<sup>(1,6-9)</sup> that provide information of volumetric organ motion associated with respiration rate, increase accuracy of target localization and can define an internal target volume [ITV]<sup>(1,8)</sup>. In previous studies<sup>(6-13)</sup>, the maximum intensity projection [MIP], average intensity projection [AIP], and mid-position [MidP] from 4DCT images were suggested for SBRT treatment planning. Furthermore, accuracy of patient positioning during each treatment session is critical, image-guided radiation therapy [IGRT] is necessary to confine patient positioning and estimate organ-tumor motions during the treatment<sup>(14)</sup> such as

### Correspondence to:

Ngamching B. Department of Radiation Oncology, Chulabhorn Hospital, HRH Princess Chulabhorn College of Medical Science, Chulabhorn Royal Academy, 54 Kamphaengphet 6, Talat Bang Khen, Lak Si, Bangkok 10210, Thailand.

**Phone:** +66-2-5766031-2, **Fax:** +66-2-5766020

**E-mail:** benjamas.nga@pccms.ac.th

**How to cite this article:** Sirichai R, Ngamching B, Khamfongkhrua C, Rojwatkarnjana S, Nantajit D, Tannanonta C. Comparison of Targeting Accuracy for Treatment Localization with Different CT Images of Moving Target in Thorax Region. J Med Assoc Thai 2018;101;Suppl.6: S119-S124.

Cone-beam computed tomography [CBCT]<sup>(15-17)</sup> verification. However, the accuracy for presenting reference image for patient verification before treatment delivery should be considered.

The purpose of this study was to compare the accuracy of target localization between free breath-CBCT [FB-CBCT] with the four different reconstruction techniques of reference CT images for treatment setup verification.

## Materials and Methods

### Phantom simulation

The QUASAR™ Programmable Respiratory Motion Phantom (Modus Medical Devices, London, ON) was used for simulating a patient's respiratory signal and tumor motion, as shown in Figure 1. A cylindrical cedar wood with 0.33 g/cm<sup>3</sup> of physical density, representing lung material was inserted into the phantom. A polystyrene sphere with 3 cm diameter and 0.855 g/cm<sup>3</sup> density was embedded inside the cedar wood to represent a solid tumor. The respiratory signal (1 cm amplitude and 15 breaths per minute (bpm) respiratory rate) relating to the tumor motion (2 cm craniocaudal [CC] direction) was created to oscillate the phantom.

### CT image acquisition

In this study, two image datasets, helical normal FB and 4 DCT scans were acquired using a 16-slice Brilliance Big Bore CT scanner (Philips Medical Systems, Cleveland, OH, USA) with real-time position management [RPM] system (Varian Medical Systems, Palo Alto, CA). The QUASAR™ phantom was aligned and set up to have its isocenter at the center of tumor volume. Three reference markers were attached to the surface of the phantom on the isocenter plane for verifying the isocenter position. The parameters for

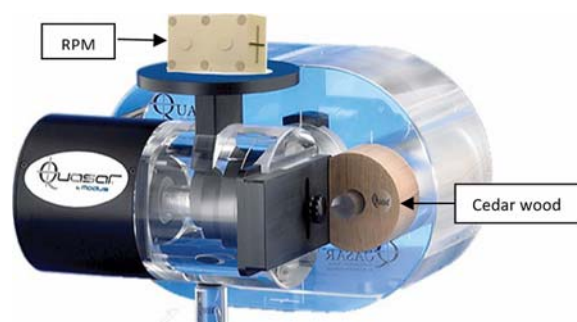


**Figure 1.** The QUASAR phantom used to simulate tumor motion.

image acquisition consisted of 3 mm slice thickness, 120 kVp, 290 mA, 512x512 matrix, 0.5 seconds per rotation and 46 cm field of view [FOV]. For the 4DCT image acquisition, a reflective marker block placed on the phantom in combination with a CCD camera was recorded by the RPM system during the CT scan. Based on RPM system, CT data acquired over the volume of interest were combined with the respiratory cycle. These images were retrospectively sorted in to ten different phase bins with the target phases of 0% to 90%<sup>(18)</sup>, such that the 0% respiratory phase corresponded to inhalation peak and the 50% respiratory phase corresponded to exhalation peak. MIP and AIP images were reconstructed from 10-phase 4DCT data in time dependent manner. MidP images were chosen from the 10-phases 4DCT images, at a time when the tumor was closest to its time-weighted mean position during the exhalation phase. All CT images (FB, MIP, AIP, and MidP) were then transferred to the radiation treatment planning system (Eclipse, version 10.0.42; Varian Medical System).

### Radiation treatment planning

All CT images were imported to the planning system. In this case, all of them were automatically registered by DICOM coordinates. The structure volume of tumor was automatically delineated by Hounsfield unit tool. The isocenter of planning was placed at the same point for every CT acquisition image. The reference images of every reconstructed technique were further transferred to the treatment room.

### CBCT image acquisition

In the treatment room, the phantom was set to be at the same position and tumor movement with the planning CT acquisition. The kV-CBCT images with free breathing [FB-CBCT] were performed using the on-board imaging [OBI] system (Varian Medical systems, Palo Alto, CA) attached to the gantry of TrueBeam linear accelerator. The scanning parameters were 3 mm slice thickness, 125kVp, 246mAs, 512x512 matrix, 16x45 cm field of view and 360° full rotation, and 60 seconds per rotation speed. Figure 2 presents the free breathing kV-CBCT images of the QUASAR™ phantom.

After the kV-CBCT scans of the phantom had been performed, the image datasets were saved to the Eclipse treatment planning system. Those images were registered automatically with the reference ones from the treatment planning by using DICOM image base. The structure volume of tumor in CBCT image was

created using the same method as the reference images (Automatic contouring). The accuracies of tumor volumes from four different reconstructed reference images were evaluated by matching with FB-CBCT image as shown in Figure 3.

### Data analysis

#### Tumor matching

The tumor matching between reference and CBCT images of all reconstructed techniques were done by five radiation oncologists. Then the accuracies of matching were analyzed by using an image matching deviation (setup deviation) and a matching index (MI). The matching index (MI) was calculated by equation (1).

$$MI = \frac{A \cap B}{A \cup B}$$

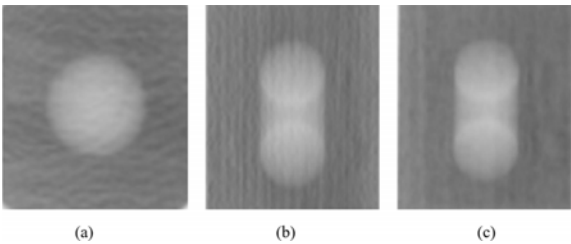


**Figure 2.** Tumor motion of 1 cm in the superior-inferior direction derived from the FB-CBCT images with (A) axial view, (B) coronal view, and (C) sagittal view.

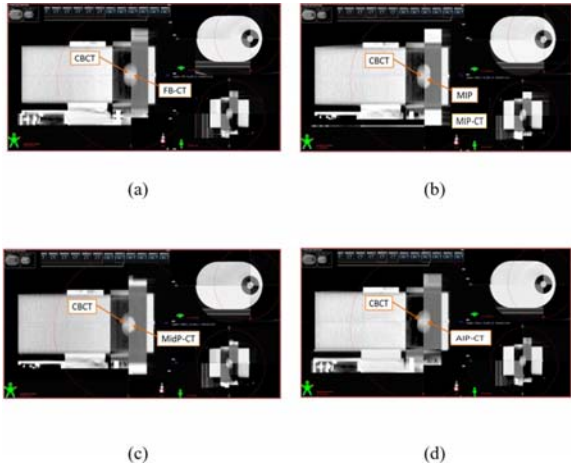


**Figure 3.** Investigation of tumor matching accuracy between (A) FB-CBCT and FB-CT, (B) FB-CBCT and MIP-CT, (C) FB-CBCT and MidP-CT, (D) FB-CBCT and AIP-CT images.

where A and B are the target volumes defined in the reference and CBCT image datasets, respectively.

If the MI value is 1, the target volume acquired from the planning CT and CBCT images are identical, and if it is 0, the target volume derived from both modalities has totally no overlapping region.

#### Image quality

In this study, the qualities of four reference images were verified based on the visualization of relevant structures by various observers (five radiation oncologists and five radiation therapists). The observers stated their opinions on the visibility of each particular structure. Evaluated criterion was categorized into one-to-five visual grading scores, as shown in Table 1.

Additionally, the visualization of target shapes derived from the CBCT and reference images of all techniques were observed to evaluate the tumor matching accuracy of ten observers. All observers compared the display shape of target structure on CBCT images with regards to the reference ones; 4DCT. The scoring used to determine the observer decision can be graded using the visual grading scale presented in Table 2.

### Results

Image matching deviation of target positioning was calculated for four reconstruction images in CC direction as shown in Table 3. The result shows the highest setup deviation according to the MidP images with the mean value of  $3.11 \pm 0.65$  mm (2.00 to 4.30 mm range), and the statistically significant deviation was found only in MidP image acquisition ( $p < 0.01$ ).

The matching indices [MI] obtained from four reconstruction methods were presented in Table 4. We

**Table 1.** Visual grading analysis for determination of image quality

Scoring	Visual grading analysis
1	Poor image quality: image not usable
2	Restricted image quality: relevant limitations for clinical use, clear loss of information
3	Sufficient image quality: moderate limitations for clinical use but no loss of information
4	Good image quality: minimal limitations for clinical use
5	Excellent image quality: no limitations for clinical use

**Table 2.** Visual grading analysis to compare target shape between CBCT images and reference images in all the reconstruction techniques

Score	Visual grading analysis
1	The tumor shape in the test image is clearly inferior to the reference image
2	The tumor shape in the test image is somewhat inferior to the reference image
3	Indecisive
4	The tumor shape in the test image is somewhat equal to the reference image
5	The tumor shape in the test image is clearly equal to the reference image

**Table 3.** Setup deviation in the superior-inferior direction using reference images obtained from the four reconstruction techniques

Reference image	Mean $\pm$ SD (mm)	Range (mm)
FB	0.68 $\pm$ 0.35	0.10 to 1.20
MIP	0.67 $\pm$ 0.49	0.00 to 1.70
MidP	3.11 $\pm$ 0.65	2.00 to 4.30
AIP	0.76 $\pm$ 0.47	0.10 to 1.60

found that the MI values from both of FB and AIP image datasets were 0.87 and 0.86, respectively. Considering all reference CT image acquisitions, the MIP image acquisition overestimated the actual volume at 0.63 MI.

The mean values of the reference image quality from all reconstruction methods are shown in Table 5. The highest score was found in MIP (3.8 $\pm$ 0.78) and AIP (3.8 $\pm$ 0.63) image datasets.

From visual assessment, the average deviation of tumor shape scores between CBCT and reference CT images by ten observers from four reconstruction techniques were displayed in Table 6. We found that the tumor shape score of CBCT was mostly equal to the reference images except in the MidP but the highest score was 3.9 $\pm$ 0.74 and 3.9 $\pm$ 0.73 for FB and AIP image acquisitions, respectively and the lowest value was also found in MidP image datasets.

## Discussion

The result shows the highest statistically significant setup deviation ( $p<0.01$ ) according to the MidP images because of the blurring effect of the images. Moreover, the MI of MIP image acquisition

**Table 4.** Matching indices defined using Eq. (1) for each reference image acquisition

Reference image	Volume (cm <sup>3</sup> )		MI
	$A \cap B$	$A \cup B$	
FB	22.65	25.92	0.87
MIP	22.81	36.02	0.63
MidP	16.92	23.53	0.72
AIP	22.71	26.46	0.86

**Table 5.** Scores of image quality for each reference image dataset

Reference image	Mean $\pm$ SD
FB	3.3 $\pm$ 0.82
MIP	3.8 $\pm$ 0.78
MidP	2.4 $\pm$ 1.26
AIP	3.8 $\pm$ 0.63

**Table 6.** Comparisons of the display shape scoring between CBCT and all reference image acquisitions

Reference image	Mean $\pm$ SD
FB	3.9 $\pm$ 0.74
MIP	3.8 $\pm$ 0.63
MidP	1.6 $\pm$ 0.70
AIP	3.9 $\pm$ 0.73

overestimated the actual volume than other datasets. But we found the target volumes acquired of AIP from CT and CBCT images was identical in Table 4.

For 5 grading score of image quality (Table 5), the MIP and AIP show the best image quality with the value of 3.8 $\pm$ 0.78 and 3.8 $\pm$ 0.63, respectively and the lowest value of the MidP (2.4 $\pm$ 1.26). This reason may be due to motion artifact effect in the geometrical time-weighted mean tumor position (rapid velocity of tumor motion region). This result agrees with the visual assessment, the tumor shape of CBCT mostly equaled reference images except in MidP image with the highest scores of close to 4 in FB and AIP image acquisitions.

Tian et al<sup>(10)</sup> compared the dosimetric of FB-CT in twenty SBRT lung cancer patients with two datasets of MIP and AVG [AIP] images. Their result shows that the dosimetric characteristics of AIP plan were similar to those of FB plan with slightly better

target volume coverage and significantly better in low-dose region in lung observed in MIP plans. AIP seemed to be favorable for planning and dose calculation of lung SBRT. Oechsner et al<sup>(11)</sup> investigated the dosimetric impact of different 4 CT datasets for lung and liver SBRT. The result shows the larger dose differences in MIP plans and similar doses in AIP and MidV. Both studies support our analyses that AIP dataset is suitable for planning and CBCT matching in terms of setup deviation and image quality for the treatment of early staged non-small cell lung cancer.

### Conclusion

Generally, the FB image datasets are used as a reference image to compare with FB-CBCT images in daily treatment. Although the MIP and AIP images have previously been evaluated to improve dose calculation accuracy for moving target, they are hardly used as a reference image for registration with the CBCT images in the treatment room. Based on the results of this study, the target volume delineated from both of FB and AIP image datasets correlated with the one from CBCT images; therefore, both FB and AIP image datasets can be used as the reference image in lung region with tumor motion in CC direction less than 2 cm. However, the respiratory rate of patient may affect the quality of on-line CBCT images; further study performed in patients is desirable.

### What is already known on this topic?

In generally, for early stage of non-small cell lung cancer radiation therapy by using free breathing planning computed tomography [FB] and maximum intensity projection [MIP] are the optimal methods for ITV delineation and treatment. And mostly investigate in dosimetric for planning but were not focus on which is the suitable dataset for matching with free-breath cone beam computed tomography [FB-CBCT] in treatment room

### What this study adds?

In this study, we show that the results of AIP image dataset and FB image dataset had better image quality for CBCT matching and contouring than other datasets presently used for early-stage non-small cell lung cancer irradiation. Both AIP and FB image datasets can be used as the reference image in lung region with tumor motion in CC direction less than 2 cm.

### Acknowledgements

The authors would like to extend our special

thanks to staff at Chulabhorn Hospital, Chulabhorn Royal Academy for their kind assistance and support towards the success and accomplishment of this research study.

### Potential conflicts of interest

The authors declare no conflicts of interest.

### References

1. Keall PJ, Mageras GS, Balter JM, Emery RS, Forster KM, Jiang SB, et al. The management of respiratory motion in radiation oncology report of AAPM Task Group 76. *Med Phys* 2006;33:3874-900.
2. Chen QS, Weinhaus MS, Deibel FC, Ciezki JP, Macklis RM. Fluoroscopic study of tumor motion due to breathing: facilitating precise radiation therapy for lung cancer patients. *Med Phys* 2001;28:1850-6.
3. Ruschin M, Sixel KE. Integration of digital fluoroscopy with CT-based radiation therapy planning of lung tumors. *Med Phys* 2002;29:1698-709.
4. Lagerwaard FJ, Van Sornsen de Koste JR, Nijssen-Visser MR, Schuchhard-Schipper RH, Oei SS, Munne A, et al. Multiple "slow" CT scans for incorporating lung tumor mobility in radiotherapy planning. *Int J Radiat Oncol Biol Phys* 2001;51:932-7.
5. Chinneck CD, McJury M, Hounsell AR. The potential for undertaking slow CT using a modern CT scanner. *Br J Radiol* 2010;83:687-93.
6. Colgan R, McClelland J, McQuaid D, Evans PM, Hawkes D, Brock J, et al. Planning lung radiotherapy using 4D CT data and a motion model. *Phys Med Biol* 2008;53:5815-30.
7. Glide-Hurst CK, Chetty IJ. Improving radiotherapy planning, delivery accuracy, and normal tissue sparing using cutting edge technologies. *J Thorac Dis* 2014;6:303-18.
8. Harada K, Katoh N, Suzuki R, Ito YM, Shimizu S, Onimaru R, et al. Evaluation of the motion of lung tumors during stereotactic body radiation therapy (SBRT) with four-dimensional computed tomography (4DCT) using real-time tumor-tracking radiotherapy system (RTRT). *Phys Med* 2016;32:305-11.
9. Deshpande S. To study tumor motion and planning target volume margins using four dimensional computed tomography for cancer of the thorax and abdomen regions. *J Med Phys* 2011;36:35-9.



10. Tian Y, Wang Z, Ge H, Zhang T, Cai J, Kelsey C, et al. Dosimetric comparison of treatment plans based on free breathing, maximum, and average intensity projection CTs for lung cancer SBRT. *Med Phys* 2012;39:2754-60.
11. Oechsner M, Odersky L, Berndt J, Combs SE, Wilkens JJ, Duma MN. Dosimetric impact of different CT datasets for stereotactic treatment planning using 3D conformal radiotherapy or volumetric modulated arc therapy. *Radiat Oncol* 2015;10:249.
12. Wolthaus JW, Sonke JJ, van Herk M, Damen EM. Reconstruction of a time-averaged midposition CT scan for radiotherapy planning of lung cancer patients using deformable registration. *Med Phys* 2008;35:3998-4011.
13. Protik A, van Herk M, Witte M, Sonke JJ. The impact of breathing amplitude on dose homogeneity in intensity modulated proton therapy. *Phys Imaging Radiat Oncol* 2017;3:11-6.
14. Chang JY, Dong L, Liu H, Starkschall G, Balter P, Mohan R, et al. Image-guided radiation therapy for non-small cell lung cancer. *J Thorac Oncol* 2008;3:177-86.
15. Guckenberger M. Image-guided radiotherapy based on kilovoltage cone-beam computed tomography—A review of technology and clinical outcome. *Eur Oncol Haematol* 2011;7:121-4.
16. Li Y, Ma JL, Chen X, Tang FW, Zhang XZ. 4DCT and CBCT based PTV margin in Stereotactic Body Radiotherapy(SBRT) of non-small cell lung tumor adhered to chest wall or diaphragm. *Radiat Oncol* 2016;11:152.
17. Sonke JJ, Rossi M, Wolthaus J, van Herk M, Damen E, Belderbos J. Frameless stereotactic body radiotherapy for lung cancer using four-dimensional cone beam CT guidance. *Int J Radiat Oncol Biol Phys* 2009;74:567-74.
18. Hugo G, Vargas C, Liang J, Kestin L, Wong JW, Yan D. Changes in the respiratory pattern during radiotherapy for cancer in the lung. *Radiation Oncol* 2006;78:326-31.
19. Ludewig E, Richter A, Frame M. Diagnostic imaging—evaluating image quality using visual grading characteristic (VGC) analysis. *Vet Res Commun* 2010;34:473-9.